Available online at www.sciencedirect.com
SCIENCE DIRECT
Biochimica et Biophysica Acta 1758 (2006) 206–212
BIOCHIMICA ET BIOPHYSICA ACTA
BBA
http://www.elsevier.com/locate/bba

A divalent-ion binding site on the 16-kDa proton channel from *Nephrops norvegicus*—revealed by EPR spectroscopy

Tibor Páli [a,1], Malcolm E. Finbow [b], Derek Marsh [a,*]

[a] *Max-Planck-Institut für biophysikalische Chemie, Abteilung Spektroskopie, 37070 Göttingen, Germany*
[b] *School of Biological and Biomedical Sciences, Glasgow Caledonian University, Glasgow, G4 0BA, UK*

Received 11 November 2005; received in revised form 20 January 2006; accepted 7 February 2006
Available online 28 February 2006

Abstract

As purified from the hepatopancreas of *Nephrops norvegicus*, the 16-kDa proton channel proteolipid is found to contain an endogenous divalent ion binding site that is occupied by Cu^{2+}. The EPR spectrum has *g*-values and hyperfine splittings that are characteristic of type 2 Cu^{2+}. The copper may be removed by extensive washing with EDTA. Titration with Ni^{2+} then induces spin–spin interactions with nitroxyl spin labels that are attached either to the unique Cys^{54}, or to fatty acids intercalated in the membrane. Paramagnetic relaxation enhancement by the fast-relaxing Ni^{2+} is used to characterise the binding and to estimate distances from the dipolar interactions. The Ni^{2+}-binding site on the protein is situated around 14–18 Å from the spin label on Cys^{54}, and is at a similar distance from a lipid chain spin-labelled on the 5 C-atom, but is more remote from the C-9 and C-14 positions of the lipid chains.

Keywords: 16-kDa proteolipid; Vacuolar ATPase; Proteolipid subunit c; Spin label; Cu^{2+}; Saturation transfer EPR

1. Introduction

The 16-kDa channel proteolipid from the hepatopancreas of *Nephrops norvegicus* bears a strong sequence identity with the proton-conducting subunit *c* of the transmembrane V_o-sector of the vacuolar V-ATPases [1]. The 16-kDa monomer is thought to traverse the membrane as a four-helix bundle [1,2]. In sarcosyl-extracted plasma membranes, the protein forms two-dimensional arrays of hexameric complexes of paired membranes [1,3]. Together with mutational analysis in yeast [4], these structures have contributed to current models for the V_o-sector in the V-ATPases. This arrangement is similar to the homologous bacterial form of the Na^+-pumping V_o-sector [5].

The crystals of the bacterial form of subunit *c* (16-kDa proteolipid) are free of metal [5] although previously it was found that the V-ATPase is inhibited by an organotin compound, which binds specifically to the *Nephrops* 16-kDa proteolipid [6]. In the present work, we use EPR spectroscopy to characterise a divalent metal ion binding site that we find in the 16-kDa protein. As purified from *Nephrops*, this site is occupied by endogenous copper and is shown to have an EPR spectrum typical of type 2 Cu^{2+}-proteins. The endogenous copper can be removed only by extensive washing with EDTA. The vacant divalent ion site could then be titrated with Ni^{2+}, and the proximity to nitroxyl spin labels – either on the unique Cys^{54} of the second transmembrane segment, or attached to the chains of intercalated lipid probes – could be investigated via the mutual spin–spin interactions by using non-linear EPR. This provides direct structural information on the arrangement of the ion binding site within the hexameric complex. Previously, we have used spin-relaxation enhancements induced by Ni^{2+} ions in the aqueous phase to determine the depth at which spin-

Abbreviations: V-ATPase, vacuolar H^+-ATPase; 5-MSL, 3-maleimido-2,2,5,5-tetramethylpyrrolidine-*N*-oxyl; *n*-SASL, *n*-(4,4-dimethyloxazolidine-*N*-oxyl)stearic acid; HEPES, 4-(2-hydroxyethyl)-1-piperazineethanesulfonic acid; EDTA, ethylenediamine tetraacetic acid; EPR, electron paramagnetic resonance; ST-EPR, saturation transfer EPR; V_1, first-harmonic absorption EPR spectrum detected in phase with respect to the static magnetic field modulation; V_2', second-harmonic absorption EPR spectrum detected 90°-out-of-phase with respect to the static magnetic field modulation

* Corresponding author. Tel.: +49 551 201 1285; fax: +49 551 201 1501.
E-mail address: dmarsh@gwdg.de (D. Marsh).
[1] Permanent address: Institute of Biophysics, Biological Research Center, H-6701 Szeged, Hungary.

0005-2736/$ - see front matter © 2006 Elsevier B.V. All rights reserved.
doi:10.1016/j.bbamem.2006.02.004

labelled residues on the 16-kDa proteolipid are located in the membrane [7].

The metallobiology of extrinsic copper-binding proteins has attracted increasing interest in recent years, partly because of their possible involvement in the pathology of neurodegenerative diseases ([8], and references therein), or in the physiological function of, for example, prion proteins [9]. Investigation of copper association with the vacuolar-ATPase proteolipid subunit, although not yet connected with either health or disease, is nonetheless of potential interest for similar reasons.

2. Materials and methods

2.1. Materials

Spin-labelled stearic acids (*n*-SASL) were synthesised according to ref. [10]. Spin-labelled maleimide (5-MSL) was obtained from Syva (Palo Alto, CA). Membranes containing the 16-kDa channel proteolipid were isolated from the hepatopancreas of the decapod *Nephrops norvegicus* by detergent extraction with Triton X-100 and *N*-lauryl sarcosine as described previously [2,11,12]. After extraction, the enriched membranes were digested with trypsin and suspended in 6 M urea before separation on sucrose step gradients. The 16-kDa proteolipid constitutes greater than 90% of the protein present and is the only protein that is labelled by maleimide in these membranous preparations [2,7].

2.2. Spin labelling

All buffers and sample capillaries used in non-linear EPR experiments were carefully deoxygenated and saturated with argon. Membranes were first washed extensively with 10 mM HEPES, 10 mM NaCl, 10 mM EDTA (pH 7.8) to remove endogenous copper. For spin labelling the lipid environment, the nitroxyl derivative of stearic acid, *n*-SASL, was added with vortexing from a stock solution in ethanol (ca. 1 mg/ml) at a level of approximately 0.5 mol% relative to membrane lipid, such that the resulting ethanol concentration was no greater than 1%. The mixture was incubated at room temperature overnight and then the membranes pelletted by centrifugation at 6000 rpm in a Biofuge (Beckmann Instruments, Palo Alto, CA). The pellets (ca. 2 mg protein) were resuspended in 60 μl of buffer, loaded into 1 mm-diameter glass capillaries which were then centrifuged and the excess supernatant removed to give samples with a height of 5 mm, according to the standard protocol for saturation transfer EPR measurements [13]. The capillaries were then flame sealed and transferred to the ESR spectrometer.

For covalent spin-labelling with the nitroxyl maleimide derivative, the 16-kDa protein was reacted by adding ca. 2 mM 5-MSL from concentrated ethanol solution (10 mg/ml), and then incubating the membrane dispersion (1–5 mg/ml) for ca. 1 h at room temperature. Unbound label was removed by repeated washing with fresh buffer. After removal of unbound label, membranes were progressively washed in buffer containing the required (cumulative) amount of $NiCl_2$ or Ni-EDTA, by mixing with a thin glass needle and centrifuging three times in the EPR capillary for each new addition of Ni^{2+} , without removing the membrane pellet between washes. ST-EPR spectra were recorded after each resuspension of the membranes in the required Ni-containing buffer. Otherwise, samples were treated as for membranes doped with the spin-labelled lipid. In the experiment depicted in Fig. 3 below, $NiCl_2$ was added in small aliquots so that interference from free Ni^{2+} was minimal. This required a large number of additions (i.e., washing steps) to achieve saturation. In titrations with larger aliquots, corrections had to be made for the relaxation induced by unbound Ni^{2+} (cf., ref. [7]).

2.3. EPR spectroscopy

EPR spectra were recorded on a Varian Century-Line 9-GHz spectrometer with rectangular TE_{102} resonator. For Cu^{2+} EPR spectra, untreated membranes were contained in a standard quartz EPR tube that was immersed in a liquid–nitrogen finger dewar. The static magnetic field was measured with a Bruker ER 035 M NMR magnetometer and the microwave frequency with a Hewlett-Packard 5345A/5355A frequency counter.

For spin-label EPR spectra, sample capillaries were accommodated in standard quartz EPR tubes containing light silicone oil for thermal stability. Temperature regulation was achieved by thermostatted nitrogen gas with a quartz flow-through dewar. Temperature was measured by a fine-wire thermocouple situated close to the sample in the silicone oil.

For recording ST-EPR spectra, the microwave H_1-field at the sample (H_1=0.25 G) was calibrated against nominal microwave power and cavity Q, as described earlier [14]. All measurements were carried out under critical coupling conditions, with a scan range of 100 G, unless indicated otherwise. After phase setting by the self-null method, ST-EPR spectra (V_2'-display) were recorded with 50 kHz field modulation, a modulation amplitude of 5.0 G and 100 kHz phase-quadrature detection [15]. Both V_1- and V_2'-spectra were corrected either with a linear baseline or with a blank spectrum from a non-labelled sample. The first integral of the V_2'-signal was normalised by the second integral of the V_1-signal (conventional first-derivative ESR spectrum) recorded at the same microwave power, but with a field modulation of 1.25 G, to give the normalised saturation transfer intensity, I_{ST} [16]:

$$I_{ST} = \frac{\int V_2'(H) \cdot dH}{\iint V_1(H) \cdot d^2H} \quad (1)$$

where integration is over the entire spectral scan width, and both V_2'- and V_1-amplitudes are normalised to the respective gains and modulation amplitudes. This standardized quantity has the advantage that values of I_{ST} are additive in multi-component ST-EPR spectra, with weightings directly representing the relative populations [16].

Simulations of powder EPR spectra were performed with the WINEPR SymFonia software from Bruker Spectrospin.

3. Results and discussion

3.1. Copper EPR spectrum

The low-temperature EPR spectrum of 16-kDa proteolipid membranes purified from the hepatopancreas of *Nephrops norvegicus* is shown in Fig. 1. These membranes have not been

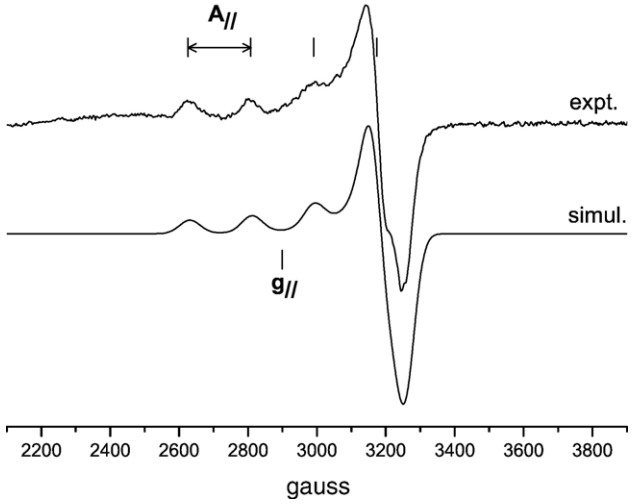

Fig. 1. Upper: Endogenous Cu^{2+} EPR spectrum of native 16-kDa proteolipid membranes purified from the hepatopancreas of *Nephrops norvegicus*. T=77 K; microwave frequency=9.1735 GHz. Lower: Spectrum simulated with the spin Hamiltonian parameters given in the text.

pre-washed with EDTA before recording the spectrum. This endogenous EPR spectrum has axial g-values $g_{//}=2.259\pm0.006$ and $g_{\perp}=2.058$, and hyperfine splitting constant $A_{//}=(190\pm8)\times10^{-4}$ cm^{-1} that are characteristic of type 2 Cu^{2+} ions (cf. refs. [17,18]). The degree of covalent ligand admixture with the Cu^{2+}, that is deduced from these measurements, is characterised by a value of α^2 ~0.85 (see ref. [19]). Such Cu^{2+} EPR spectra are typical of coordination with nitrogen and oxygen ligands, and are found on binding Cu^{2+} to simple peptides and to both endogenous and extrinsic sites in a variety of proteins [17,18].

Fig. 2 gives a plot of $A_{//}$ vs. $g_{//}$ for various small-molecule Cu^{2+}-complexes, using data from the literature. The dependence of $A_{//}$ on $g_{//}$ correlates with the type of ligands in the complexes [18,20]. The EPR data from Cu^{2+} bound to the 16-kDa proteolipid fall in a region encompassed by imidazyl ligands, and are next closest to those for square-planar Cu^{2+}-complexes with 4 oxygen ligands, although the possibility of 2 nitrogens and 2 oxygens certainly cannot be excluded. Liganding to four imidazyl nitrogens (shown by the open squares in Fig. 2) is unlikely as a candidate structure, because the 16-kDa protein has only a single, non-conserved histidine residue, His^{93}. Coordination to the latter residue, which is located in the third transmembrane segment, could be possible. Simultaneous coordination by histidines from two 16-kDa molecules, however, would require an unusual alignment of adjacent monomers in the hexameric assemblies. A system of oxygen ligands analogous to that reported recently for Na^+ binding to the corresponding V-type Na-ATPase subunit from *Enterococcus hirae* [5] is not possible because sequence alignment shows that only Glu^{140} (*Nephrops* numbering) is common to the *Nephrops* proteolipid.

It is possible that the Cu^{2+} binding site on the 16-kDa proteolipid may be extrinsic and that the Cu^{2+} ions are picked up from the arthropod haemocyanin, on purification. Nonetheless, the EPR spectrum corresponds to a well-defined axial site for divalent transition metal ions and is only removed after extensive washing with millimolar EDTA. As will be seen below, this site can alternatively be occupied by Ni^{2+}.

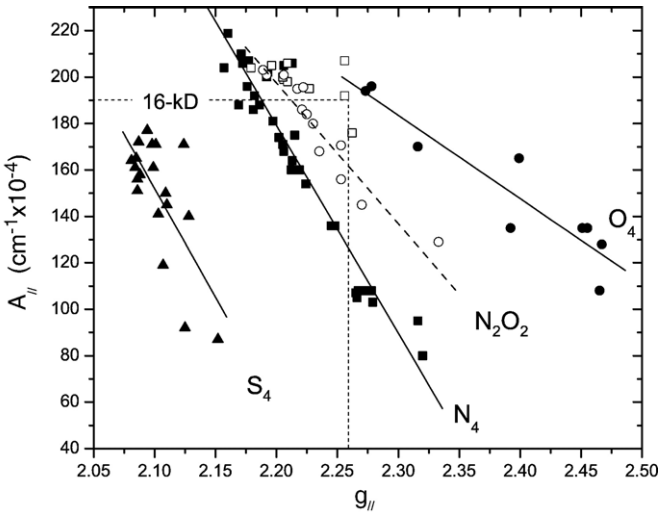

Fig. 2. Correlation diagram between $A_{//}$ and $g_{//}$ in the EPR spectra of Cu^{2+} complexes with different ligands: ■ four nitrogen ligands (N_4), ● four oxygen ligands (O_4), ▲ four sulphur ligands (S_4), ○ two nitrogen and two oxygen ligands (N_2O_2), □ imidazyl-type N_4 ligands. References to original data are in refs. [18] and [20]. Dashed horizontal and vertical lines indicate the parameters for Cu^{2+} bound to the 16-kDa proteolipid.

3.2. Spin-label ST-EPR spectral intensities in the presence of Ni^{2+}

Purified membranes containing the 16-kDa proteolipid were washed extensively with 10 mM EDTA, until the endogenous Cu^{2+} EPR signal was no longer visible (see Materials and methods). Spin-labelling was then performed either with the 5-MSL sulphydryl reagent, or by intercalating different positional isomers of the stearic acid spin label, *n*-SASL, in the lipid phase of the membrane. In this way, it is possible to look at the interaction both between the metal and a label covalently attached to the protein, and between labels in the bilayer and the bound metal. The ST-EPR spectra of the membranous 16-kDa proteolipid labelled specifically on Cys^{54} with the maleimide derivative 5-MSL have been characterised previously [7]. Conventional EPR spectra of the *n*-SASL lipid spin labels intercalated in 16-kDa membranes have also been presented previously [3].

Spin–spin interactions (in this case, static dipolar) with fast-relaxing paramagnetic ions such as Ni^{2+} alleviate saturation of spin-label EPR spectra in the non-linear (i.e., partially saturating) regime. This results in a reduction in intensity of the ST-EPR spectra of the spin label (see, e.g., ref. [21]). Because the reciprocal of the integrated ST-EPR intensity, $1/I_{ST}$, is related approximately linearly to the spin-lattice relaxation rate of the spin label, we use this to quantitate the paramagnetic relaxation enhancement induced by Ni^{2+} ions (see also refs. [21,22]).

Quenching of the ST-EPR spectrum from intercalated 5-SASL by progressive addition of Ni^{2+} to 16-kDa membranes from which Cu^{2+} has been removed is shown in Fig. 3. The reciprocal normalised integral intensity, $1/I_{ST}$, of the ST-EPR spectrum is given as a function of the number of times that the membranes were resuspended in fresh aliquots of 0.2 mM $NiCl_2$ (see Materials and methods). Representative ST-EPR spectra for increasing numbers of resuspensions in $NiCl_2$ are given in the insert to Fig. 3. The concentration of $NiCl_2$ was chosen such that any unbound Ni^{2+} ions remaining in the aqueous phase would have a negligible effect on the ST-EPR intensities (cf. ref. [7]). It is seen from Fig. 3 that the ST-EPR intensity of the 5-SASL spin label decreases progressively with the number of Ni^{2+}-washing steps, finally reaching a limiting value after approximately 40 steps. This progression corresponds to saturable binding of Ni^{2+} ions to the membranes. The decrease in ST-EPR intensity arises from enhancement of the spin-label relaxation by paramagnetic spin–spin interactions with the bound Ni^{2+} ions (see e.g. ref. [21]). The total binding capacity corresponds approximately to the region of 0.05–0.1 μmole Ni^{2+} ions per mg protein. This value is determined by extrapolating the linear binding region in Fig. 3, at low Ni^{2+} concentrations, to the saturation value.

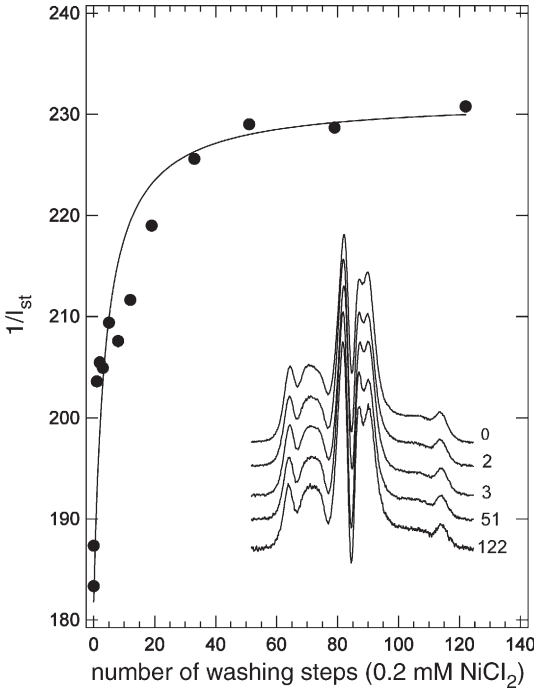

Fig. 3. Dependence of the reciprocal normalised ST-EPR intensity, $1/I_{ST}$, of 16-kDa proteolipid membranes, extensively washed with EDTA and labelled with 5-SASL, on the number of subsequent additions of 0.2 mM $NiCl_2$ (see Materials and methods for details). Inset: ST-EPR spectra for increasing numbers of washing steps with 0.2 mM $NiCl_2$, as indicated. $T=5$ °C.

3.3. Ni^{2+} binding curves from ST-EPR

A more standard type of Ni^{2+} binding experiment is shown in Fig. 4. In these close-packed membranous proteolipid preparations, binding of paramagnetic metal ions to the protein can be detected by spin–spin interactions either with a protein-bound spin label (5-MSL) or with a spin label attached to a lipid (*n*-SASL). Fig. 4 shows the ST-EPR spectra of 5-MSL or 5-SASL for 16-kDa membranes suspended in different concentrations of $NiCl_2$. Spin–spin interactions result in a progressive decrease of overall spectral intensity with increasing Ni^{2+} concentration. The decrease in intensity takes place without appreciable change in the ST-EPR lineshapes (except for the complete quenching of a small, sharp, mobile component at the isotropic resonance position in the spectra of 5-MSL).

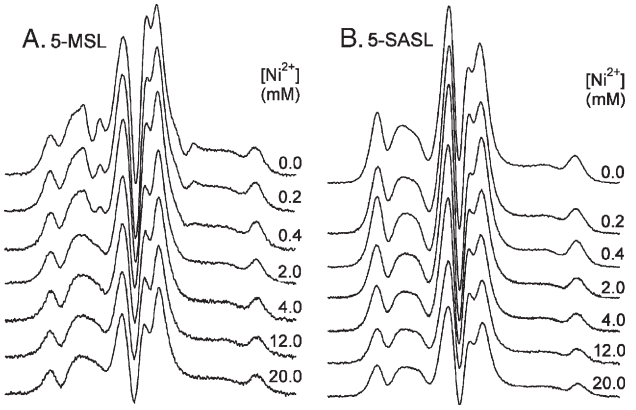

Fig. 4. ST-EPR spectra of 16-kDa proteolipid membranes spin-labelled with (A) 5-MSL or (B) 5-SASL, and suspended in the concentrations of $NiCl_2$ indicated. The integrated height of the spectra is scaled to reflect the normalised integrated intensity, I_{ST}, defined by Eq. (1). Total scan width = 100 gauss; $T=5$ °C.

The reciprocal ST-EPR intensity, $\delta(1/I_{ST})$, for both 5-MSL and the *n*-SASL lipid labels, is plotted in Fig. 5 as a function of increasing concentration of added Ni^{2+} ions. However, in order to compensate for paramagnetic relaxation enhancement by free Ni^{2+} ions in the aqueous phase, a sloping baseline obtained by linear regression of the data points at high Ni^{2+} concentration has been subtracted from the original experimental data for $1/I_{ST}$ in this titration (cf. ref. [7]). This procedure is unavoidable, but unfortunately magnifies the scatter in the data. Saturation binding of Ni^{2+} corresponds to the $\delta(1/I_{ST})=0$ level in Fig. 5. The data given by the squares in Fig. 5 correspond to the addition of Ni^{2+} complexed to EDTA. These latter data all scatter about the zero level, because chelated Ni^{2+} in the Ni-EDTA complex is unable to bind to the protein. All other data in Fig. 5 refer to addition of free Ni^{2+}, in the absence of EDTA.

Half-saturation of the reduction in ST-EPR intensity of 5-MSL occurs at ca. 0.5 mM Ni^{2+} added, and the binding is still approximately linear in this region, i.e., essentially all the Ni^{2+} added becomes bound. Therefore the binding constant for the Ni^{2+} site is well into the sub-millimolar range. This binding is much stronger than the intrinsic affinity of Ni^{2+} ions for phospholipid membranes (see ref. [23]). Phosphatidylcholine is the major lipid of *Nephrops* 16-kDa membranes, with relatively

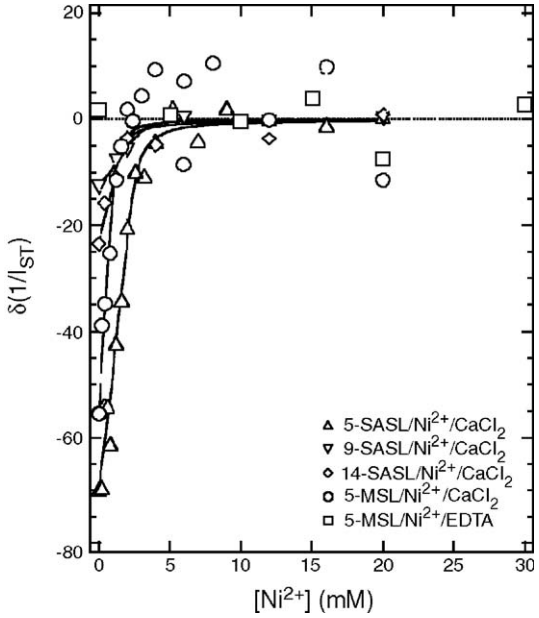

Fig. 5. Dependence of the reciprocal normalised ST-EPR integral intensity, $\delta(1/I_{ST})$, on aqueous Ni^{2+} ion concentration for 16-kDa proteolipid membranes either specifically labelled with 5-MSL (circles or squares), or spin-labelled in the lipid regions of the membranes with various *n*-SASL stearic acid spin probes (upward and downward triangles, and diamonds). Baselines have been subtracted from linear regressions of $1/I_{ST}$ for $[Ni^{2+}] \geq 4$ mM to yield the low-concentration increment $\delta(1/I_{ST})$. The data for 5-MSL that are given by squares correspond to the Ni-EDTA complex, all other data correspond to free aqueous Ni^{2+}. $T=5$ °C.

little aminophospholipids [3]; and Ni^{2+} does not display high-affinity binding to phosphatidylcholine membranes [24]. Qualitatively similar conclusions can be reached from the data for 5-SASL in Fig. 5. The extent of paramagnetic quenching for the latter is comparable to that for 5-MSL, whereas for 9-SASL and 14-SASL the quenching is weaker. Confirmation that the effects arise from direct binding of Ni^{2+} ions comes from comparison with the results obtained with the complex of Ni^{2+} with EDTA that was referred to above.

Eliminating the effects of relaxation by free Ni^{2+} ions, as is done in Fig. 5, yields a normalised ST-EPR intensity, $I_{ST}(f_b)$, that is subject to paramagnetic relaxation enhancement only by the bound Ni^{2+} ions:

$$I_{ST}(f_b) = (1 - f_b)I_{ST,f} + f_b I_{ST,b} \quad (2)$$

where $I_{ST,b}$ is the (normalised) ST-EPR intensity of a spin label on the protein with bound Ni^{2+}, $I_{ST,f}$ is that in the absence of Ni^{2+}, and f_b is the fraction of proteins to which Ni^{2+} is bound. The latter can be expressed in terms of the association constant, K, for binding of Ni^{2+}, by using the law of mass action:

$$f_b = K(1 - f_b)([Ni^{2+}]/[P] - f_b) \quad (3)$$

where $[Ni^{2+}]$ is the total Ni^{2+} concentration and [P] is the total concentration of protein. The baseline-corrected reciprocal ST-EPR intensity introduced above is given by:

$$\delta(1/I_{ST}) = 1/I_{ST}(f_b) - 1/I_{ST,b} \quad (4)$$

Combination of Eqs. (2)–(4) then describes the binding curves that are given in Fig. 5. Of the data given for the different spin labels in Fig. 5, only those for 5-SASL have low enough scatter for least-squares analysis, and this yields an approximate association constant for Ni^{2+} of $K \approx 1.5 \times 10^4\ M^{-1}$. The binding curves for the other spin labels are consistent with this value, to within experimental error. However, this value may well be a considerable underestimate, because the high protein concentrations required for ST-EPR measurements limit the precision of binding-constant determinations. The stability constant is, nevertheless, approaching those for single amino acids or peptides [25], and the lower affinity sites on some proteins [8].

Data for the Ni^{2+}-quenching of the ST-EPR intensities from intercalated *n*-SASL spin-labelled fatty acids are compared with those for 5-MSL in Fig. 5. In the case of 5-SASL, which is spin-labelled in the upper part of the lipid chain, very similar results are obtained to those with 5-MSL attached to Cys^{54}. For other positions of labelling in the lipid chain, 9-SASL and 14-SASL, the effects of Ni^{2+} binding are considerably smaller. This reduction in the total change, $\delta(1/I_{ST})^o = 1/I_{ST,f} - 1/I_{ST,b}$, at saturation binding of Ni^{2+} demonstrates the positional sensitivity of the relaxation enhancements. In all cases, the Ni^{2+} titration occurs over approximately the same range, confirming that the effects observed correspond to binding to the same Ni^{2+} ion site for both covalently linked and lipid-bound spin labels. It will be noted that the spin-labelled stearic acid probes are intercalated throughout the lipid phase of the membrane and hence do not necessarily have a unique position relative to the protein subunits. However, the comparatively low lipid/protein ratio of sarcosyl-extracted membranes, and the selectivity of fatty acids for interaction with the 16-kDa protein, ensure that nearly all *n*-SASL probes are situated at the lipid–protein interface [3]. Therefore, it may be expected that all fatty acids spin-labelled at a given position in the chain will have nearly comparable lateral separations from the ion binding site on the corresponding 16-kDa monomer.

3.4. Estimation of the distance from the paramagnetic ion site

For a spin-label interacting with a single fast-relaxing paramagnetic ion at a distance, r, the dipolar enhancement in spin-lattice relaxation rate of the spin label can be approximated by the Solomon–Bloembergen equation (see, e.g., ref. [26]):

$$\frac{1}{T_{1,dd}} = \frac{4}{3} g_R^2 \beta_e^2 S_R(S_R + 1)\gamma_e^2 T_{1,R} \cdot \frac{1}{r^6} \quad (5)$$

where g_R, S_R and $T_{1,R}$, respectively, are the g-value, spin and spin-lattice relaxation time of the paramagnetic relaxant, and β_e and γ_e are the electron Bohr magneton and the gyromagnetic ratio of the spin label, respectively. Assuming that the intensity, I_{ST}, of the ST-EPR spectrum is linearly proportional to the spin-lattice relaxation time of the spin label [22,27], the increment, $|\delta(1/I_{ST})^o|$, at saturation of the ion binding site is given by (see e.g. ref. [21]):

$$|\delta(1/I_{ST})^o| = (T_1^o/I_{ST}^o)(1/T_{1,dd}) \quad (6)$$

where T_1^o and I_{ST}^o are the spin-lattice relaxation time and value of I_{ST}, respectively, of the spin label in the absence of paramagnetic ions. Combination of Eqs. (5) and (6) then allows estimation of the distance of the paramagnetic ion-binding site from the spin label.

The spin-lattice relaxation time of the bound Ni^{2+} ions is not known with certainty, but the values for hexa-aquo Ni^{2+}: $g_R = 2.25$, $T_{1,R} = 2.9 \times 10^{-12}$ s, $S_R = 1$ [28] can be taken for the purpose of estimation. Assuming that $T_1^o \sim 2$–10 μs for the spin label (see, e.g., ref. [21]) then leads to a value of $r \sim 14$–18 Å for the distance from the covalently bound 5-MSL spin label. Corresponding distances from the *n*-SASL spin labels are $r \sim 14$–18 Å, 17–23 Å and 16–21 Å for 5-SASL, 9-SASL and 14-SASL, respectively. The relatively short separation from 5-SASL indicates that a Ni^{2+} binding site is associated with each monomer of the 16-kDa hexamer, which is consistent with the approximate binding capacity.

These results show that the Cu^{2+} binding site is situated relatively close, and at comparable distances, to the spin labels on Cys^{54} and on 5-SASL, but more remotely from 9-SASL and 14-SASL. This conclusion is consistent with findings that the spin label on Cys^{54} is accessible to spin-labelled lipids and also is situated at a vertical position that is closer to that of 5-SASL than that of 9-SASL (or 14-SASL) [7]. The proximity to Cys^{54} suggests that the Cu^{2+} site is probably located towards the cytosolic side of the membrane (for a V-ATPase). According to current models of the 16-kDa protein assembly, the present estimates of distance from Cys^{54} on transmembrane segment 2 and from lipid suggest that the divalent ion site is situated more

in the region of the outer transmembrane segments 2 and 4, than of the N-terminal transmembrane segment 1 and analogous segment 3 that are located towards the interior of the hexamer [4,29]. Note that the diameter of a close-packed α-helix is ~10 Å and that of a close-packed lipid chain is ~5 Å. Thus, the minimum (i.e., radial) distance from a spin-labelled lipid to the mid-point of the proteolipid ring is already ~10–15 Å. Such an arrangement with the binding site not directly exposed to water would, however, require compensation of the ionic charge.

The location of the divalent ion appears to be in a highly conserved region, possibly close to the extramembranous loops between transmembrane helices 1 and 2, and transmembrane helices 3 and 4, that interface with the stalk subunit of the V_1-sector of the V-ATPase, indicating that other forms of subunit *c* might also bind to Cu^{2+} and/or Ni^{2+}. As isolated, the arrays of 16-kDa proteolipid are paired membranes and these 2 extra-membranous loops form the basis of the end-to-end association, which possibly might be expected to impede their accessibility to metal. However, uranyl and phosphotungstate salts are both known to penetrate the small space between apposing membranes [30]. Therefore, it cannot be excluded that the metal binding site might be the result of the end-to-end associations of apposing 16-kDa proteolipids and thus be absent in the fully assembled V-ATPase.

4. Conclusions

An exchangeable divalent ion site, which is occupied by endogenous Cu^{2+}, is found in the 16-kDa proteolipid V-ATPase-like subunit from *Nephrops norvegicus*. The binding site most likely involves at least two oxygen ligands, or one histidine, and not more than two non-histidine nitrogen ligands, in an approximately square-planar arrangement. This site is situated closer to Cys^{54} and the C5 position of the lipid chains than to the C9 and C14 fatty acid chain positions. This places it potentially in the outer regions of the cytoplasmic leaflet of the vacuolar membrane, possibly in the outer ring of transmembrane helices. At present, the possible function of this copper binding site is not known, but it cannot be excluded that it might be involved in some way with copper homeostasis.

Acknowledgements

We thank Frau Brigitta Angerstein for spin label synthesis and expert technical assistance, and Ms. Pauline McLean and Mrs. M. Scott for the preparation of *Nephrops* membranes. This work was supported in part by contract no. QLG-CT-2000-01801 of the European Commission and by the Hungarian National Science Fund (OTKA T043425 to T.P.).

References

[1] A. Holzenburg, P.C. Jones, T. Franklin, T. Páli, T. Heimburg, D. Marsh, J.B.C. Findlay, M.E. Finbow, Evidence for a common structure for a class of membrane channels, Eur. J. Biochem. 213 (1993) 21–30.

[2] M.E. Finbow, E.E. Eliopoulos, P.J. Jackson, J.N. Keen, L. Meagher, P. Thompson, P.C. Jones, J.B.C. Findlay, Structure of 16 kDa integral membrane protein that has identity to the putative proton channel of the vacuolar H^+-ATPase, Protein Eng. 5 (1992) 7–15.

[3] T. Páli, M.E. Finbow, A. Holzenburg, J.B.C. Findlay, D. Marsh, Lipid–protein interactions and assembly of the 16-kDa channel polypeptide from *Nephrops norvegicus*. Studies with spin-label electron spin resonance spectroscopy and electron microscopy, Biochemistry 34 (1995) 9211–9218.

[4] P.C. Jones, M.A. Harrison, Y.I. Kim, M.E. Finbow, J.B.C. Findlay, The first putative transmembrane helix of the 16 kDa proteolipid lines a pore in the V-0 sector of the vacuolar H^+-ATPase, Biochem. J. 312 (1995) 739–747.

[5] T. Murata, I. Yamato, Y. Kakinuma, A.G.W. Leslie, J.E. Walker, Structure of the rotor of the V-type Na^+-ATPase from *Enterococcus hirae*, Science 308 (2005) 654–659.

[6] G. Hughes, M.A. Harrison, Y.I. Kim, D.E. Griffiths, M.E. Finbow, J.B.C. Findlay, Interaction of dibutyltin-3-hydroxyflavone bromide with the 16 kDa proteolipid indicates the disposition of proton translocation sites of the vacuolar ATPase, Biochem. J. 317 (1996) 425–431.

[7] T. Páli, M.E. Finbow, D. Marsh, Membrane assembly of the 16-kDa proteolipid channel from *Nephrops norvegicus* studied by relaxation enhancements in spin-label ESR, Biochemistry 38 (1999) 14311–14319.

[8] R.M. Rasia, C.W. Bertoncini, D. Marsh, W. Hoyer, D. Cherny, M. Zweckstetter, C. Griesinger, T.M. Jovin, C.O. Fernández, Structural characterization of copper(II) binding to α-synuclein: insights into the bioinorganic chemistry of Parkinson's disease, Proc. Natl. Acad. Sci. U. S. A. 102 (2005) 4294–4299.

[9] G.L. Millhauser, Copper binding in the prion protein, Acc. Chem. Res. 37 (2004) 79–85.

[10] W.L. Hubbell, H.M. McConnell, Molecular motion in spin-labelled phospholipids and membranes, J. Am. Chem. Soc. 93 (1971) 314–326.

[11] M.E. Finbow, T.E.J. Buultjens, N.J. Lane, J. Shuttleworth, J.D. Pitts, Isolation and characterisation of arthropod gap junctions, EMBO J. 3 (1984) 2271–2278.

[12] T.E.J. Buultjens, M.E. Finbow, N.J. Lane, J.D. Pitts, Tissue and species conservation of the vertebrate and arthropod forms of the low molecular weight (16–18000) proteins of gap junctions, Cell Tissue Res. 251 (1988) 571–580.

[13] M.A. Hemminga, P.A. De Jager, D. Marsh, P. Fajer, Standard conditions for the measurement of saturation transfer ESR spectra, J. Magn. Reson. 59 (1984) 160–163.

[14] P. Fajer, D. Marsh, Microwave and modulation field inhomogeneities and the effect of cavity Q in saturation transfer ESR spectra. Dependence on sample size, J. Magn. Reson. 49 (1982) 212–224.

[15] P. Fajer, A. Watts, D. Marsh, Saturation transfer, continuous wave saturation, and saturation recovery electron spin resonance studies of chain-spin labeled phosphatidylcholines in the low temperature phases of dipalmitoyl phosphatidylcholine bilayers. Effects of rotational dynamics and spin–spin interactions, Biophys. J. 61 (1992) 879–891.

[16] L.I. Horváth, D. Marsh, Analysis of multicomponent saturation transfer ESR spectra using the integral method: application to membrane systems, J. Magn. Reson. 54 (1983) 363–373.

[17] T. Vänngård, Copper proteins, in: H.M. Swartz, J.R. Bolton, D.C. Borg (Eds.), Biological Applications of Electron Spin Resonance, Wiley-Interscience, New York, 1972, pp. 411–447.

[18] J. Peisach, W.E. Blumberg, Structural implications derived from analysis of electron paramagnetic resonance spectra of natural and artificial copper proteins, Arch. Biochem. Biophys. 265 (1974) 691–708.

[19] D. Kivelson, R. Neiman, ESR studies on the bonding in copper complexes, J. Chem. Phys. 35 (1961) 149–155.

[20] U. Sakaguchi, A.W. Addison, Spectroscopic and redox studies of some copper(II) complexes with biomimetic donor atoms—Implications for protein copper centers, J. Chem. Soc. Dalton Trans. 4 (1979) 600–608.

[21] D. Marsh, T. Páli, L.I. Horváth, Progressive saturation and saturation transfer EPR for measuring exchange processes and proximity relations in membranes, in: L.J. Berliner (Ed.), Spin Labeling, The Next Millenium, vol. 14, Plenum Press, New York, 1998, pp. 23–82.

[22] T. Páli, V.A. Livshits, D. Marsh, Dependence of saturation-transfer EPR intensities on spin-lattice relaxation, J. Magn. Reson., B 113 (1996) 151–159.

[23] D. Marsh, Handbook of Lipid Bilayers, CRC Press, Boca Raton FL; 1990.
[24] T. Páli, R. Bartucci, L.I. Horváth, D. Marsh, Distance measurements using paramagnetic ion-induced relaxation in the saturation transfer electron spin resonance of spin-labeled biomolecules. Application to phospholipid bilayers and interdigitated gel phases, Biophys. J. 61 (1992) 1595–1602.
[25] R.M.C. Dawson, D.E. Elliot, W.H. Elliot, K.M. Jones, Data for Biochemical Research, Oxford Univ. Press, Oxford; 1969.
[26] I. Bertini, C. Luchinat, NMR of Paramagnetic Molecules in Biological Systems, Benjamin/Cummings, Menlo Park, CA; 1986.
[27] D. Marsh, L.I. Horváth, A simple analytical treatment of the sensitivity of saturation transfer EPR spectra to slow rotational diffusion, J. Magn. Reson. 99 (1992) 323–331.
[28] H.L. Friedman, M. Holz, H.G. Hertz, EPR relaxations of aqueous Ni^{2+} ion, J. Chem. Phys. 70 (1979) 3369–3383.
[29] M.A. Harrison, J. Murray, B. Powell, Y.I. Kim, M.E. Finbow, J.B.C. Findlay, Helical interactions and membrane disposition of the 16-kDa proteolipid subunit of the vacuolar H^+-ATPase analyzed by cysteine replacement mutagenesis, J. Biol. Chem. 274 (1999) 25461–25470.
[30] B. Leitch, M.E. Finbow, The gap junction-like form of a vacuolar proton channel component appears not to be an artifact of isolation—An immunocytochemical localization study, Exp. Cell Res. 190 (1990) 218–226.